

PACS numbers: 42.65.Yj; 42.65.Re
DOI: 10.1070/QE2009v039n07ABEH014177

Optical parametric amplification of X-shaped localised wave-packets

A. Dubietis, V. Smilgevičius, A. Stabinis, G. Valiulis, A. Piskarskas

***Abstract*. The general concepts for generation and amplification of the X-pulses in optical parametric amplifiers under the plane-wave and localised (Bessel beam, or more generally, X-pulse) pump are reviewed. It is shown numerically and experimentally that X-pulse phase-matching gives rise to spontaneous emergence of the localised light structures in the regime of the parametric frequency down-conversion. The parametric amplification technique of localised waves is extended to the chirped X-pulse optical parametric amplification concept, which allows one to achieve few optical cycle, high-peak power localised wave packets for laser – matter interactions.**

Keywords: *parametric amplification, X-pulses, localised wave packets.*

1. Introduction

The first theoretical concepts of the optical parametric amplification and oscillation were introduced in theoretical works by Akhmanov and Khokhlov [1], Kroll [2], and Kingston [3] dating back to early 1960s. Soon these concepts were applied to proof-of-principle demonstration of the optical parametric amplifiers [4, 5] and wavelength tunable optical parametric oscillators [6, 7]. This field of research rapidly grew to maturity and the first picosecond optical parametric amplifier (OPA) was launched in 1968 [8]. Actually, it resulted in extended studies of ultrafast OPAs aiming at the development of frequency-tunable sources of the ultrashort light pulses with a duration approaching few optical cycles (see reviews [9, 10]). An exclusive feature of parametric interactions in transparent crystals with a quadratic nonlinearity $\chi^{(2)}$ is a large gain bandwidth [11, 12], in principle allowing the generation of the light pulses much shorter than the pump pulse. In particular, the broad amplification bandwidth of the OPA is provided by the noncollinear interaction geometry, which was first pointed out by Gale et al. [13]. This capability as combined with a new optical parametric chirped pulse amplification (OPCPA) concept [14 – 16] holds a promise to scale the performance of the conventional ultrafast lasers down to single optical cycle pulse generation and to boost the output power to the multi-petawatt level [17, 18]. Noncollinear phase matching of the X-pulses opens an innovative approach to control and shape the OPA gain bandwidth [19]. X-pulses expose strong angular-frequency dependence and hold unique features of dispersion-free and diffraction-free propagation. Moreover, X-shaped spatio-temporal spectrum emerges as a result of the interplay between the temporal dispersion and spatial diffraction in the OPA [20, 21]. An important conclusion was made demonstrating for the first time that the conditions for noncollinear phase matching in three-wave parametric interactions coincide with the conditions for the generation and amplification of the focus wave modes (X-pulses or, in general, localised waves) [20]. The results of experiments on generation of ultrabroadband localised optical fields by the optical parametric amplification are quite promising and further investigations are in progress. Recently, the X-pulse OPCPA concept has been suggested in [22] introducing a new straight method to compress amplified X-pulses down to a few tens of femtoseconds by free propagation of chirped X-pulse in vacuum. This approach excludes expensive components of an optical compressor routinely used in high intensity laser systems.

In this paper, we study the phase-matching requirements for the three X-wave parametric interactions and discuss the experimental results on the X-wave generation in the OPA. We also propose an idea of the optical parametric amplification of chirped X-pulses and demonstrate analytical and numerical results obtained quite recently, which might open new perspectives in amplification of high peak power ultrashort laser pulses.

A. Dubietis, V. Smilgevičius, A. Stabinis, G. Valiulis, A. Piskarskas
Department of Quantum Electronics, Vilnius University, Saulėtekio Ave. 9, bldg. 3, LT-10222 Vilnius, Lithuania;
e-mail: algis.piskarskas@ff.vu.lt

Received 12 March 2009
Kvantovaya Elektronika **39** (7) 599 – 608 (2009)
Submitted in English

2. Optical X-pulses

Generation of localised, propagation-invariant wave-packets, which withstand diffractive and dispersive broadening while propagating in a free space or in a dispersive medium, is one of the most urgent and exciting problems in modern optics. At present, localised waves attract considerable attention from the fundamental point of view as well as suggest an innovative approach in many practical applications [23]. While the Bessel beam is well known for being the simplest monochromatic localised wave, which exhibits diffraction-free propagation [24], the X-pulse (or sometimes called X-wave) represents the generalisation of the concept of energy localisation in space and time in the case of polychromatic beams carrying ultrashort light pulses [25].

The optical X-pulse constitutes a weakly localised wave-packet exhibiting an exceptional feature of coexistence of a localised high-intensity core and a high energy, but low intensity beam periphery (energy reservoir), which propagates locally as a single (quasi)-stationary profile. In its simplest form, a linear X-pulse represents a propagation-invariant wave packet, which is the solution of paraxial propagation equation in a dispersive medium:

$$\frac{\mathrm{i}\partial A}{\partial z}+\frac{g_0}{2}\frac{\partial^2 A}{\partial t^2}-\frac{1}{2k_0}\Delta_\perp A=0, \tag{1}$$

where A is the complex electrical field amplitude; $\Delta_\perp$ is the transverse Laplace operator; $g_0=\mathrm{d}^2k/\mathrm{d}\omega^2|_{\omega_0}$ is the group velocity dispersion (GVD) coefficient; and $k_0=\omega_0 n(\omega_0)/c$ is the propagation constant. In the space–time domain, a propagation-invariant wave packet takes the shape of the letter 'X' – with the intense and highly localised central spike and slowly decaying tails (Fig. 1). In a dispersive medium, the propagation-invariant wave packet (X-pulse) emerges whenever its spatiotemporal spectrum in the $(k_\perp,\Delta\omega)$ domain asymptotically fits the dispersion relation:

$$\alpha=g_0\Delta\omega^2-k_\perp^2/k_0=\mathrm{const}, \tag{2}$$

where $k_\perp$ is the transverse wave-vector component related to the cone angle $\theta\approx k_\perp/k_0$ and $\Delta\omega=\omega-\omega_0$ is the frequency detuning from the carrier frequency. In the case of the normal group velocity dispersion ($g_0>0$), Eqn (2) represents a family of hyperbolas, while the angularly resolved spectral shape resembles an X-shaped profile associated with the lines along $\alpha=0$:

$$k_\perp=\pm\sqrt{k_0 g_0}\,\Delta\omega. \tag{3}$$

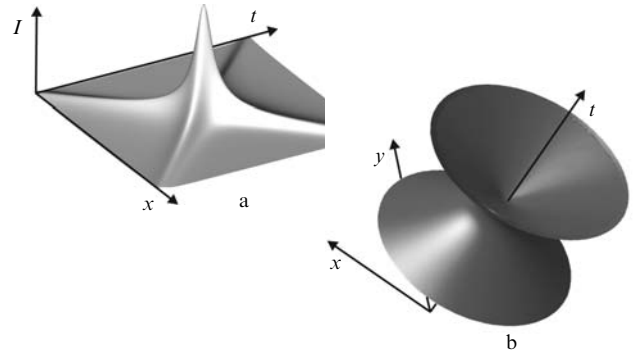

Figure 1. Spatiotemporal representation of the X-pulse: (a) spatiotemporal intensity profile $I(x,t)$, (b) iso-intensity surface at the intensity level $0.1I_{\max}$.

Therefore, the X-pulse represents a combination of coloured cones with each cone corresponding to a particular frequency. If the spectral components comprise an exponential spectrum and are phase-locked, the spatiotemporal electric field distribution takes the shape of the X-pulse [26]:

$$E(r,t)=\mathrm{Re}\left[(\Delta-\mathrm{i}t)^2+k_0 g_0 r^2\right]^{-1/2}, \tag{4}$$

where Δ is the duration of the central peak. If the spectrum of the X-pulse lies in a limited spectral domain, the X-pulse carries a limited (non-infinite) power and energy.

An interesting feature of the X-pulse is that it can be constructed to possess desirable propagation properties – group and phase velocity, energy localisation, etc., either in a free-space or in a dispersive medium [20, 27–32]. In practice, experimental methods for X-pulse generation are rapidly developing, and they are currently based on the linear optics involving axicons and holographic elements [33], microaxicons [34], beam shaping techniques [35, 36] and cylindrical gratings [37]. It is interesting to note, that the X-pulses can be generated directly from the laser resonator containing conical optical elements [38], or even emerge as modes of passively mode-locked fiber laser cavity in the presence of the normal group velocity dispersion [39].

On the other hand, X-pulses are also the solutions of nonlinear propagation equations, which involve quadratic and cubic nonlinearities [26], and spontaneously emerge in many frequently encountered problems of nonlinear optics. In media with a quadratic nonlinearity, the X-pulses are excited at phase-mismatched second harmonic generation [40–42] and parametric frequency down-conversion [19, 20, 43, 44]. In transparent media possessing the fast Kerr nonlinearity, the nonlinear X-pulses are excited via femtosecond filamentation [45–47], which opens new routes for ultrashort frequency conversion [48]. X-pulses spontaneously emerge in more specific, periodic nonlinear environments such as photonic crystals [49], waveguide arrays [50] and nonlinear lattices [51].

3. Phase-matching of the X-waves in $\chi^{(2)}$ crystals

The possibility of amplification of localised X-shaped waves in an optical parametric amplifier (OPA) was first theoretically considered in [20]. It was shown that distortion-free amplification of localised waves and X-waves, in particular, in the field of the plane-wave pump becomes possible due to simultaneous achievement of angular and spectral phase-matching requirements. In this section we extend this idea demonstrating that the phase-matching condition for the X-waves in the nonlinear crystals with the quadratic nonlinearity is very general, and could be satisfied upon pumping by a plane wave and Bessel beam or an X-wave. More importantly, we show that in the regime of parametric frequency down-conversion, localised waves emerge spontaneously, as demonstrated by numerical simulations and first experimental results.

3.1 General considerations

An X-wave in a dispersive medium can be represented as a superposition of coaxial Bessel beams whose frequencies ω, wave vectors $\boldsymbol{k}$ and cone angles θ are related by the equation

$$k(\omega)\cos\theta(\omega)=\omega/V+\gamma, \tag{5}$$

where V is the group velocity of an X-wave, and γ is an arbitrary constant defining the angular dispersion [33]. The phase-matching conditions of interacting X-waves in a nonlinear medium with the quadratic nonlinearity $\chi^{(2)}$ can be directly obtained by using the phase-matching conditions for plane and monochromatic waves with the account for the requirement for the angular dispersion [Eqn (5)]. As a result, the phase-matching conditions of the X-waves in $\chi^{(2)}$ medium can be written in the form

$$\begin{aligned}
&\omega_1+\omega_2=\omega_3,\\
&k_1\cos\theta_1+k_2\cos\theta_2=k_3\cos\theta_3,\\
&k_1\sin\theta_1+k_2\sin\theta_2=k_3\sin\theta_3,\\
&k_j\cos\theta_j=\omega_j/V_j+\gamma_j,\ \ j=1,2,3,
\end{aligned}\tag{6}$$

where the subscripts 1, 2, 3 denote signal, idler and pump waves, respectively (Fig. 2).

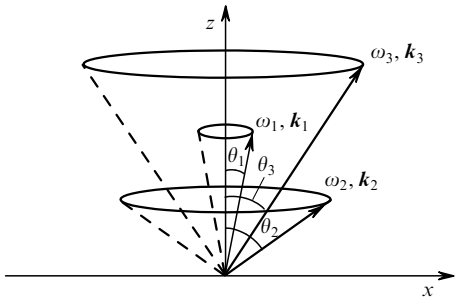

Figure 2. Scheme of the non-collinear phase-matching of three plane monochromatic waves in a nonlinear crystal.

We assume that the cone axis of the X-waves coincides with the direction of the collinear phase-matching of three plane monochromatic waves with frequencies $\omega_{10}+\omega_{20}=\omega_{30}$ and wave vectors $\boldsymbol{k}_{10}+\boldsymbol{k}_{20}=\boldsymbol{k}_{30}$, respectively. Then, according to Eqn (5), $\omega_j=\omega_{j0}+\Delta\omega_j$, $k_{j0}=\omega_{j0}/V_j+\gamma_j$ and

$$k_j\cos\theta_j=k_{j0}+\Delta\omega_j/V_j.\tag{7}$$

Now the phase-matching conditions for the X-waves take the form:

$$\begin{aligned}
&\Delta\omega_1+\Delta\omega_2=\Delta\omega_3,\\
&\Delta\omega_1/V_1+\Delta\omega_2/V_2=\Delta\omega_3/V_3,\\
&k_1\sin\theta_1+k_2\sin\theta_2=k_3\sin\theta_3,\\
&k_j\cos\theta_j=k_{j0}+\Delta\omega_j/V_j,\ \ j=1,2,3.
\end{aligned}\tag{8}$$

Further we restrict our consideration to the paraxial approximation $\sin\theta_j\approx\theta_j$, $\cos\theta_j\approx1-\theta_j^2/2$, assume that $|\Delta\omega_j|\ll\omega_{j0}$, and expand the wave vectors $\boldsymbol{k}_j$ into Taylor series

$$k_j(\omega_{j0}+\Delta\omega_j)\approx k_{j0}+\frac{\Delta\omega_j}{u_{j0}}+\frac{g_{j0}}{2}\,\Delta\omega_j^2,$$

where u_{j0} and g_{j0} are the group velocity and GVD coefficient of the jth wave with the carrier frequency ω_{j0}, respectively. In the case of noncritical phase-matching, when the lateral walk-off of the interacting waves can be neglected, the system of equations (8) can be rewritten in the form

$$\begin{aligned}
&\Delta\omega_1+\Delta\omega_2=\Delta\omega_3,\\
&\Delta\omega_1/V_1+\Delta\omega_2/V_2=\Delta\omega_3/V_3,\\
&k_{10}\theta_1+k_{20}\theta_2=k_{30}\theta_3,\\
&k_{j0}\theta_j^2=2(1/u_{j0}-1/V_j)\Delta\omega_j+g_{j0}\Delta\omega_j^2,\ \ j=1,2,3.
\end{aligned}\tag{9}$$

The solutions of Eqns (9) were analysed in detail in Ref. [19]. We will discuss below the phase-matching conditions of the X-waves for some cases of practical interest, which can be obtained under real experimental conditions.

3.2 Parametric down-conversion of a quasi-monochromatic plane wave

We assume that the pump wave is a quasi-monochromatic plane wave, therefore in Eqns (9) we set $\Delta\omega_3\approx0$, $\theta_3\approx0$. In this case, we find $\Delta\omega_1=-\Delta\omega_2=\Delta\omega$, $V_1=V_2=V$ (group velocity matching), and

$$k_{10}\theta_1+k_{20}\theta_2=0,\tag{10}$$

$$k_{j0}\theta_j^2=2(1/u_{j0}-1/V)\Delta\omega_j+g_{j0}\Delta\omega_j^2,\ \ j=1,2.\tag{11}$$

When the cone axis of the X-waves in the nonlinear crystal coincides with the direction of phase-matched degenerate type I parametric interaction ($\omega_{10}=\omega_{20}=\omega_0=\omega_{30}/2$ and $\boldsymbol{k}_{10}=\boldsymbol{k}_{20}=\boldsymbol{k}_0=\boldsymbol{k}_{30}/2$) the solutions of Eqns (10)–(11) have the form

$$\theta_1=-\theta_2=\theta,\ \ \theta=\pm\sqrt{g_0/k_0}\,\Delta\omega,\tag{12}$$

and $u_{10}=u_{20}=u_0=V$, $g_{10}=g_{20}=g_0$. Thus, the angular dispersion curves of the parametrically amplified X-waves in the degenerate OPA pumped by a plane monochromatic wave are represented by two intersecting straight lines.

If the cone axis of the X-waves in the nonlinear crystal coincides with the direction of phase-matched non-degenerate parametric interaction ($\omega_{10}\neq\omega_{20}$), the term with $\Delta\omega_j^2$ can be neglected, and Eqn (11) can be rewritten in the form

$$k_{j0}\theta_j^2=2(1/u_{j0}-1/V)\Delta\omega_j,\ \ j=1,2.\tag{13}$$

Now the non-diffracting propagation of the amplified signal and idler waves ($V=\text{const}$) takes place at the group velocity

$$V=\frac{k_{30}u_{10}u_{20}}{k_{10}u_{20}+k_{20}u_{10}}=\text{const}.\tag{14}$$

In this case, the angular dispersion curves of the amplified X-waves are described by hyperbolas:

$$\begin{aligned}
&\theta_1^2=(2/k_{10})(1/u_{10}-1/V)\Delta\omega,\\
&\theta_2^2=(2/k_{20})(1/u_{20}-1/V)\Delta\omega.
\end{aligned}\tag{15}$$

Figure 3 presents the angular-spectral distribution of the parametric superfluorescence experimentally measured at the output plane of an imaging spectrometer for different temperatures of type I phase-matching KDP crystal pumped by the fourth-harmonic pulses ($\lambda_3=266$ nm) from a cw mode-locked Nd : YAG laser [19]. The numerical fit of the experimental curve at the degeneracy is illustrated by intersecting straight lines in Fig. 3c, showing a good agreement between the theoretical predictions and exper-

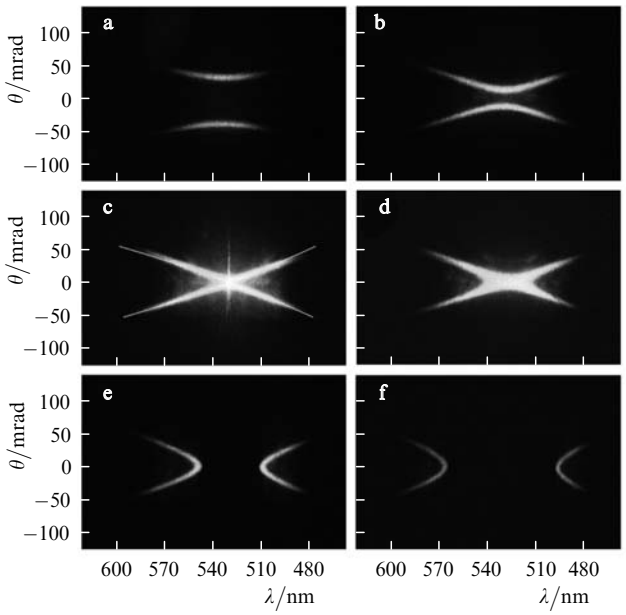

Figure 3. Angular-spectral distribution of the OPA output radiation in air measured for different KDP crystal temperatures: (a) 32 °C, (b) 56 °C, (c) 60 °C, (d) 60.5 °C, (e) 68 °C, (f) 76 °C; $\lambda_3 = 266$ nm. The numerical fit at the degeneracy is plotted by straight lines (c). Reprinted with permission from Ref. [19].

imental results. Thus, the parametric down-conversion in the field of a quasi-monochromatic pump beam stimulates an excitation of nondiffracting pulsed signal and idler beams from the quantum noise level. These beams should obtain a typical X-shape if the components of the spatiotemporal spectrum are properly phase-locked. A particularly interesting experimental proof refers to the demonstration of the optical parametric amplification of tightly focused (highly divergent) broadband Gaussian seed signal, which reshapes into a pulsed Bessel beam as a result of spatiotemporal gain properties of the OPA [52].

3.3 Parametric down-conversion of a monochromatic Bessel beam

Now let us assume that the pump wave is a quasi-monochromatic Bessel beam with a cone angle θ_3 (see Fig. 2). The evolution of the signal wave amplitude in an OPA pumped by a Bessel beam is described by the equation

$$\frac{\partial A_1}{\partial z} = -\frac{1}{u_0}\frac{\partial A_1}{\partial t} + \mathrm{i}\,\frac{g_0}{2}\frac{\partial^2 A_1}{\partial t^2} - \mathrm{i}\,\frac{\Delta_\perp}{2k_0}\,A_1 + \mathrm{i}\sigma a_3 J_0(\beta_0 r) A_1^*. \quad (16)$$

Here, k_0, u_0 and g_0 are the wave vector, group velocity, and GVD coefficient of the signal wave at the degeneracy $\omega_0 = \omega_3/2$; σ is the nonlinear coupling coefficient; a_3 is the amplitude of the Bessel pump beam; J_0 is the zero-order Bessel function; and $\beta_0 = k_3 \sin\theta_3$ is the transverse wave vector of the pump wave. For simplicity, we assume that all the optical fields are axially symmetric.

Equation (16) was solved numerically with the parameters $\lambda_1 = 532$ nm and $\lambda_3 = 266$ nm and with the initial random signal amplitude (noise burst) A_1 at the input. The duration and the transverse size of the noise burst was taken 100 ps and 120 μm, respectively. As a nonlinear medium, we considered a temperature-tuned ADP crystal cut for the noncritical type I phase-matching. The results of the numerical simulation for three propagation distances inside the nonlinear crystal are shown in Fig. 4 [44]. Two pairs of

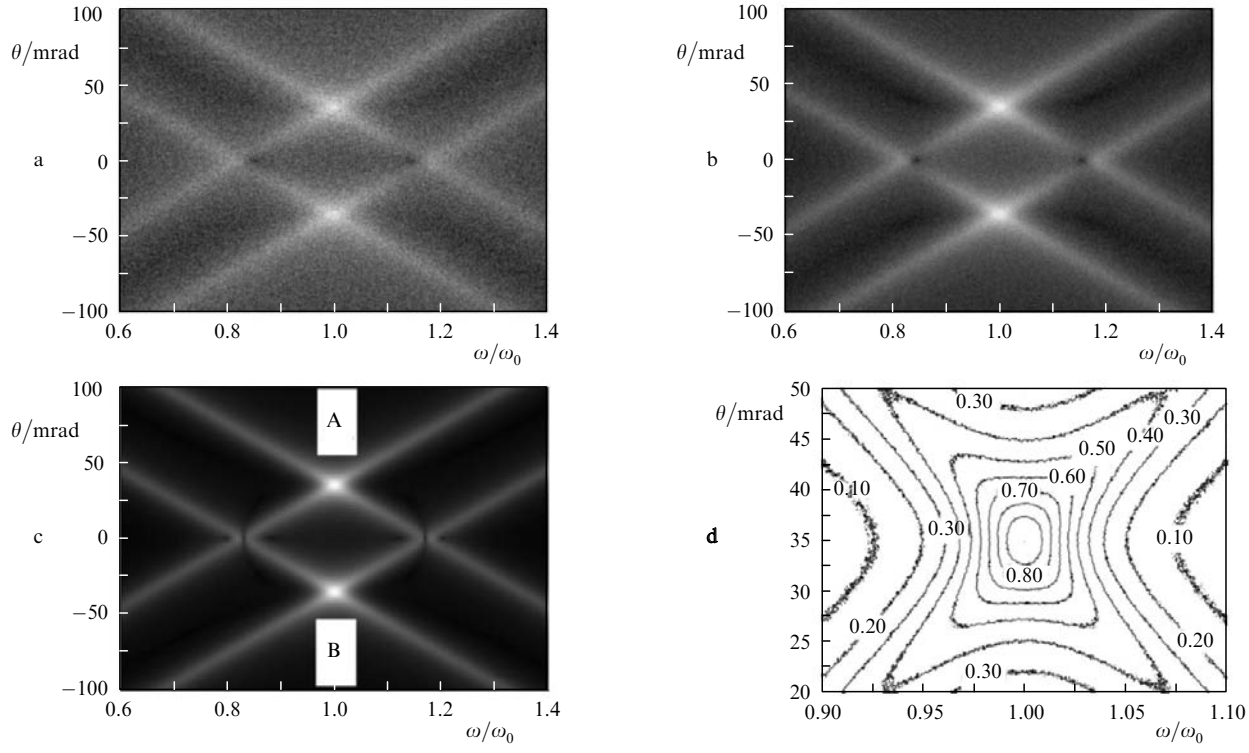

Figure 4. Frequency-resolved far-field spectra of the signal wave emerging from noise at different propagation distances in the ADP crystal: (a) 1 cm, (b) 2 cm, (c) 3 cm; (d) contour plot of the spatiotemporal intensity distribution of the signal wave at the output of the crystal. Reprinted with permission from Ref. [44].

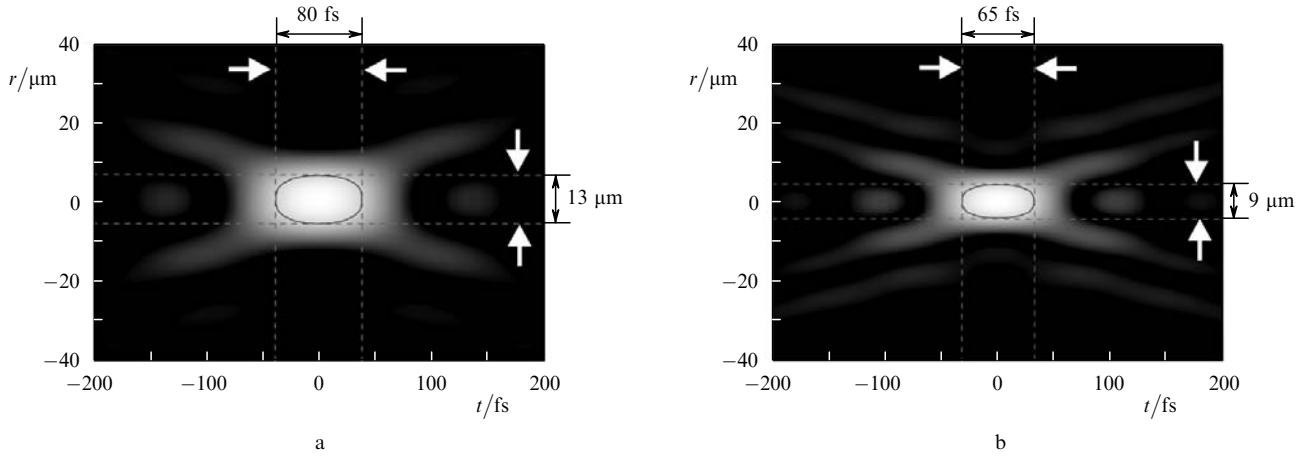

Figure 5. Spatiotemporal intensity profile of the amplified signal beam calculated for two different values of the Bessel pump beam cone angle: (a) $\theta_3 = 35$ mrad, (b) $\theta_3 = 70$ mrad. The contour line indicates the half-intensity level. Reprinted with permission from Ref. [44].

straight lines intersecting at points A and B situated on the pump cone correspond to the degenerate parametric interaction (see Fig. 4c). The numerical results are in good agreement with the theoretical predictions.

The spatiotemporal profile of the amplified signal wave at the output of the nonlinear crystal is shown in Fig. 5 [44], which resembles the familiar X-shape known from classical studies of nondiffractive and nondispersive optical fields. Apparent spatiotemporal localisation of the excited light field increases with increasing the pump Bessel beam cone angle as evident from comparison of Fig. 5a and Fig. 5b. The results suggest that an input noise burst in the OPA pumped by a quasi-monochromatic Bessel beam spontaneously reshapes into the nondiffracting X-shaped pulsed beam with a pulse duration and a beam width with a high degree of the spatiotemporal localisation. Note that the similar reshaping by the spontaneous phase-locking of the spatiotemporal components of the input spectrum is also possible in the OPA pumped by a narrow Gaussian pump beam if its diffraction could be neglected. Figure 6 shows the experimentally obtained angular-spectral distribution of the parametric superfluorescence measured at the output of the ADP crystal pumped by the Bessel beam. The crystal length was 4 cm and its temperature was 55 °C. One can see that this distribution qualitatively reproduces the main results of the numerical simulation shown in Fig. 4 [44]. Pumping was performed by the fourth-harmonic generation ($\lambda = 266$ nm) from a cw mode-locked Nd : YAG laser.

It is worth mentioning that the spontaneous phase-locking in the amplified noise signal was observed under different experimental conditions. The occurrence of the azimuthal correlation in the noise signal amplified in the OPA pumped by a narrow Gaussian beam with a ring-shaped gain profile was demonstrated in Ref. [53]. In this case, the probability of the Bessel beam excitation increased with decreasing the pump beam diameter. The radial inhomogeneity of the parametric gain caused by the central peak of the Bessel beam can also stimulate the appearance of radial coherence of the optical field excited from the quantum noise level [54].

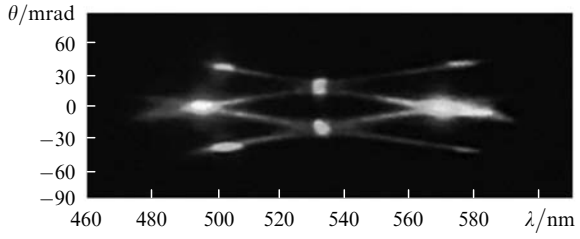

Figure 6. Experimentally measured frequency-resolved far-field spectrum of the signal wave excited in the ADP crystal by the Bessel pump beam. Reprinted with permission from Ref. [44].

3.4 Parametric amplification of quasi-monochromatic plane signal wave

If we assume that the signal is a quasi-monochromatic plane wave ($\Delta\omega_1 \approx 0$, $\theta_1 \approx 0$), then the phase-matching conditions [Eqns (9)] take a form:

$$k_{20}\theta_2 = k_{30}\theta_3, \tag{17}$$

$$k_{j0}\theta_j^2 = 2(1/u_{j0} - 1/V)\Delta\omega, \quad j = 2, 3, \tag{18}$$

where $V = V_2 = V_3$; $\Delta\omega = \Delta\omega_2 = \Delta\omega_3$. The non-diffracting propagation of the pump and idler waves occurs at the group velocity

$$V = \frac{k_{10}u_{20}u_{30}}{k_{30}u_{20} - k_{20}u_{30}}. \tag{19}$$

The angular dispersion curves for pump and idler X-waves should be the hyperbolas

$$\theta_3^2 = (2/k_{30})(1/u_{30} - 1/V)\Delta\omega,$$
$$\theta_2^2 = -(2/k_{20})(1/u_{20} - 1/V)\Delta\omega. \tag{20}$$

Note that in this case, the coherent parametric amplification of the axial signal wave is also possible by the incoherent pump wave whose angular dispersion obeys the requirement for the non-diffracting propagation. This idea might be extended by considering a multicolour conical wave to pump the OPA and to convert the energy from the incoherent radiation into the coherent one, exposing the cumulative action, known as energy combining [55, 56].

4. Optical parametric amplification of chirped X-pulses

The chirped pulse amplification (CPA) technique allows one to amplify an ultrashort optical pulse without distortions of spectral, spatial and phase characteristics. An ultrashort (e.g. broadband) optical pulse is stretched in time by decreasing its peak power, amplified without the onset of intensity-dependent beam or pulse self-action effects. Then, the pulse is again re-compressed to the original duration, retaining its high peak power. The OPCPA technique, which replaces a laser amplifier by the optical parametric amplifier, was proposed in 1992 by some of the present authors [14] and nowadays serves as a tool for developing of modern high-peak power ultrashort pulse laser systems [17].

In this section we consider the foundations of the chirped X-pulse optical parametric amplification in the field of a plane pump wave (or more generally, extended Gaussian beam) [22]. By selecting a suitable temporal chirp at the input X-pulse, the amplified chirped X-pulse is re-compressed to its original duration during its propagation in the free space (vacuum) at the position of the target and, therefore, does not require a complex arrangement of the pulse compressor.

4.1 Properties of chirped X-pulses

The concept of the chirped X-pulse (CXP) as a specific wave packet was first introduced in paper [29]. Unlike conventional chirped Gaussian pulses, which recover only their temporal shape after passing the pulse compressor, chirped X-pulses recover their entire spatial and temporal shape after propagating some distance in a dispersive medium. In other words, the chirped X-pulse is not propagation invariant; nevertheless its spatial and temporal characteristics can be constructed in such a way so that to obtain a high-quality beam in the irradiation of the target.

In what follows, we discuss some basic and specific properties of chirped X-pulses. Propagation of a radially symmetric wave packet in linear dispersive medium under paraxial approximation is described by the equation

$$\frac{\partial A}{\partial z} + v\,\frac{\partial A}{\partial \eta} - \frac{\mathrm{i}}{2}\,g_0\,\frac{\partial^2 A}{\partial \eta^2} + \frac{\mathrm{i}}{2k_0}\,\Delta_\perp A = 0, \tag{21}$$

where $A(r,\eta,z)$ is the complex amplitude; $\eta = t - z/V$ is the retarded time; x, y are transverse and z is longitudinal coordinates, respectively; $v = 1/u_0 - 1/V$ is the group velocity mismatch with respect to the reference frame moving with velocity V. One of the possible non-stationary solutions of Eqn (21) possessing an arbitrary angular dispersion $\delta(\omega)$ is

$$A(r,\eta,z) = \frac{1}{2\pi}\int_{-\infty}^{\infty} S_0(\omega) J_0(\delta(\omega) r)$$

$$\times \exp\left[\frac{z}{2\mathrm{i}k_0}\left(k_0 g_0 \omega^2 + 2k_0 v\omega - \delta^2(\omega)\right)\right] \exp(\mathrm{i}\omega\eta)\mathrm{d}\omega, \tag{22}$$

where $S_0(\omega)$ is the spectrum of the initial pulse at $z = 0$ and $r = 0$. The spectral phase remains constant with propagation if $\delta(\omega) = (k_0 g_0 \omega^2 + 2k_0 v\omega)^{1/2}$, and the solution of Eqn (22) is the X-pulse with propagation-invariant envelope moving with the group velocity . Its axial ($r = 0$) amplitude is simply defined by the temporal spectrum $S(\omega)$ at the input and is expressed as

$$A(0,\eta,z) = \frac{1}{2\pi}\int_{-\infty}^{\infty} S_0(\omega)\exp(\mathrm{i}\omega\eta)\mathrm{d}\omega. \tag{23}$$

By setting an appropriate angular dispersion relation $\delta(\omega)$ into Eqn (22), one can control the propagation dynamics of the X-pulse described by Eqn (21).

Consider now a chirped Gaussian pulse of duration τ with the amplitude

$$A_0(t) = a_0 \exp\left[-\frac{t^2}{\tau^2(1-\mathrm{i}\beta)}\right]$$

and the spectral envelope

$$S_0(\omega) = B_0 \exp\left[-\frac{\omega^2}{\Delta\omega^2}(1+\mathrm{i}\beta)\right], \tag{24}$$

where $B_0 = a_0\tau\sqrt{\pi}(1-\mathrm{i}\beta)^{-1/2}$ is the spectral amplitude; $\Delta\omega = [4(1+\beta^2)/\tau^2]^{1/2}$ is the spectral width at the 1/e level; β is the chirp parameter. By substituting Eqn (24) into Eqn (22) and for simplicity assuming the coordinate frame moving with the pulse group velocity $V = u_0$, we obtain an expression for a CXP with the Gaussian envelope at the beam center:

$$A(r,\eta,z) = \frac{B_0}{2\pi}\int_{-\infty}^{\infty} \exp\left[-\left(\frac{\omega}{\Delta\omega}\right)^2\right] J_0(\delta(\omega) r)$$

$$\times \exp\left\{-\mathrm{i}\left[\frac{\beta\omega^2}{\Delta\omega^2} + \frac{z g_0 \omega^2}{2} - \frac{z\delta^2(\omega)}{2k_0}\right]\right\} \exp(\mathrm{i}\omega\eta)\mathrm{d}\omega. \tag{25}$$

Equation (25) describes the CXP, whose on-axis behaviour is equivalent to a Gaussian pulse in the medium possessing some effective dispersion $k_{\mathrm{eff}}(\omega) = k_0 + g_0\omega^2/2 - \delta^2(\omega)/2k_0$. Figure 7 compares the spatiotemporal intensity distribution of the transform-limited ($\beta = 0$) X-pulse and CXP with $\beta = 100$ of the same duration with spectral bandwidth corresponding to 10-fs transform-limited pulse. The CXP still possess a characteristic X-shaped profile, but with sharper intensity contrast and faster decaying tails out of the beam center [22].

In what follows, assuming the angular dispersion law in the form of the quadratic polynomial with arbitrary parameters p and q (p, $q > 0$): $\delta^2(\omega) = p\omega^2 + q$, the duration of the CXP changes with propagation, and the best compression occurs at the distance

$$z_{\mathrm{c}} = \frac{2k_0\beta}{\Delta\omega^2(p - k_0 g_0)}. \tag{26}$$

The required dispersion properties of the medium for self-compression to occur follow from the sign of the chirp parameter. For $\beta > 0$, the pulse is compressed when $g_0 < p/k_0$ that can be accomplished either in the medium with a normal or anomalous GVD or in a vacuum ($g_0 = 0$). This property of the CXP is of great practical importance, because it allows one not only to control efficiently the relevant parameters of the wave-packet during propagation, but also to compress the pulse without using a complex optical arrangement.

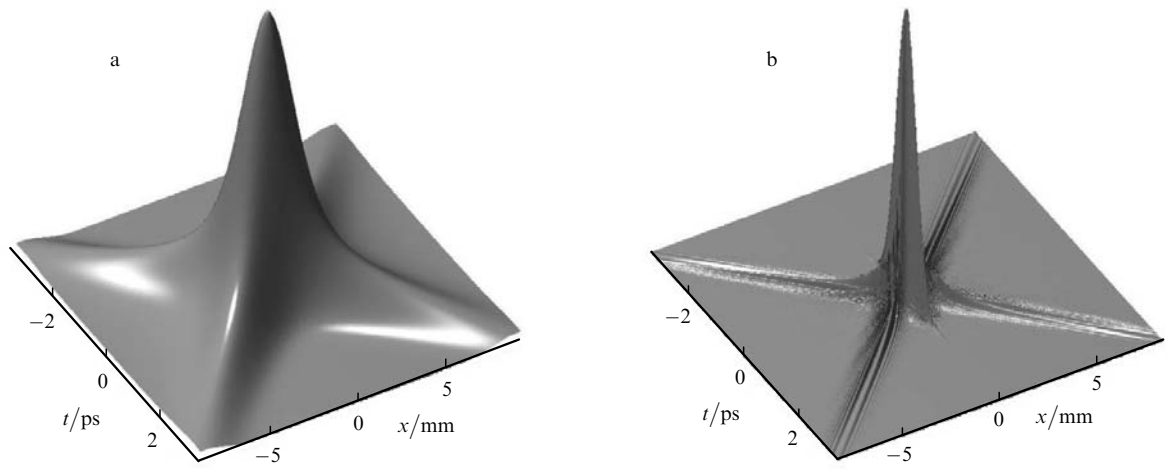

Figure 7. Spatiotemporal intensity distribution of (a) transform-limited and (b) chirped X-pulses. Axial pulse widths in both cases are identical and equal to 1 ps. Reprinted with permission from Ref. [22].

4.2 Optical parametric amplification of chirped X-pulses

Recall that the gain bandwidth of the collinear OPA within the first dispersion approximation is limited by the group velocity mismatch between the signal and idler pulses. The idea of broadband phase matching is based on imposing the angular dispersion on the spectral components and hence ensuring the exact phase-matching condition for all the frequency components comprising the pulse. For a conventional Gaussian wave packet, this modification is equivalent to tilting of the amplitude front with respect to the phase front. Thus, the group velocity of the tilted pulse in a birefringent medium is controlled by pulse-front tilt angle. More importantly, pulse-front tilting allows one to control also the sign and magnitude of the effective GVD, 'seen' by the pulse [57]. If combined together, both modifications alter pulse propagation in a dispersive medium to a great extent and might be adjusted to ensure extremely broad amplification bandwidth of the OPA. The X-pulse, on the other hand, brings the generalisation of the tilted pulse idea for the case of the cylindrical symmetry, resulting in a cylindrically symmetric wave packet with the angular dispersion. The group velocity and the effective GVD coefficient of the X-pulse are controlled in the same way as in the case of the tilted pulse [58].

Consider now optical parametric amplification of a weak CXP signal in the field of a plain monochromatic pump pulse. In the undepleted-pump approximation ($|A_1|, |A_2| \ll |A_3|$; $A_3 = \text{const} = a_3$), parametric amplification of the signal and idler waves in the coordinate frame moving with the group velocity of the pump pulse is described by the set of equations

$$\begin{aligned}
&\frac{\partial A_1}{\partial z} + v_{13}\frac{\partial A_1}{\partial \eta} - \frac{\mathrm{i}}{2}g_{10}\frac{\partial^2 A_1}{\partial \eta^2} + \frac{\mathrm{i}}{2k_{10}}\Delta_\perp A_1 = \mathrm{i}\sigma_1 A_2^* a_3,\\
&\frac{\partial A_2}{\partial z} + v_{23}\frac{\partial A_2}{\partial \eta} - \frac{\mathrm{i}}{2}g_{20}\frac{\partial^2 A_2}{\partial \eta^2} + \frac{\mathrm{i}}{2k_{20}}\Delta_\perp A_2 = \mathrm{i}\sigma_2 A_1^* a_3,
\end{aligned} \tag{27}$$

where subscripts 1, 2, 3 stand for signal, idler and pump waves, respectively; $v_{j3} = 1/u_{j0} - 1/u_{30}$ is the group velocity mismatch; the parameters g_{j0} ($j = 1, 2$) are the GVD coefficients for the signal and idler pulses, respectively; and σ_j is the nonlinear coupling coefficient. The solution of Eqn (27) has the form of a Bessel-type X-pulse with the angular dispersion:

$$A_j(r,\eta,z) = \frac{1}{2\pi}\int_{-\infty}^{\infty} S_j(\omega,z)J_0(\delta_j(\omega)r)\exp(\mathrm{i}\omega\eta)\mathrm{d}\omega, \tag{28}$$

where

$$\begin{aligned}
S_1(\omega,z) &= [S_{10}(\omega)\cosh(\Gamma(\omega)z)\\
&\quad - \mathrm{i}R_{10}(\omega)\sinh(\Gamma(\omega)z)]\exp[-\mathrm{i}D(\omega)z],\\
S_2^*(-\omega,z) &= [S_{20}^*(-\omega)\cosh(\Gamma(\omega)z)\\
&\quad + \mathrm{i}R_{20}(\omega)\sinh(\Gamma(\omega)z)]\exp[-\mathrm{i}D(\omega)z],
\end{aligned} \tag{29}$$

$$\begin{aligned}
R_{10}(\omega) &= \frac{K(\omega)S_{10}(\omega) + \sigma_1 a_3 S_{20}^*(-\omega)}{\Gamma(\omega)},\\
R_{20}(\omega) &= \frac{K(\omega)S_{20}^*(-\omega) + \sigma_2 a_3 S_{10}(\omega)}{\Gamma(\omega)},\\
\Gamma(\omega) &= \left[\sigma_1\sigma_2 a_3^2 - K^2(\omega)\right]^{1/2},\\
D(\omega) &= \frac{1}{2}[D_1(\omega) - D_2(-\omega)],\\
K(\omega) &= \frac{1}{2}[D_1(\omega) + D_2(-\omega)].
\end{aligned} \tag{30}$$

The introduced parameter $D_j(\omega) = \omega v_{j3} + \frac{1}{2}\omega^2 g_{j0} - \delta_j(\omega)^2(2k_{j0})^{-1}$ describes the evolution of the spectral phase during propagation, i.e. the so-called nonlinear dispersion, whereas the parameter $\Gamma(\omega)$ defines the spectral gain. The gain bandwidth of the parametric amplifier becomes infinite if the gain for all the spectral components is uniform: $\Gamma(\omega) = \text{const}$. This condition requires $K(\omega) = 0$, which could be satisfied by setting the angular dispersion of the CXP in the form

$$\delta_1^2(\omega) = \frac{2k_{10}k_{20}}{k_{10}+k_{20}}\left(v_{12}\omega + \frac{g_{10}+g_{20}}{2}\,\omega^2\right). \tag{31}$$

Equation (31) describes the condition of the infinite OPA gain bandwidth for the given approximation, which, in a more general case, can be extended up to any higher order dispersion approximation. The transformation of the spectral phase during propagation is defined by the parameter $D(\omega) = 0$:

$$D(\omega) = \frac{1}{k_{10}+k_{20}} \times\left[(v_{13}k_{10}+v_{23}k_{20})\omega + \frac{1}{2}(g_{10}k_{10}-g_{20}k_{20})\omega^2\right]. \tag{32}$$

Then, the solution provided by Eqn (29) with account for Eqn (31) is transformed to the form:

$$S_1(\omega,z) = \left[S_{10}(\omega)\cosh(\Gamma_0 z) - \mathrm{i}\sqrt{\frac{\sigma_1}{\sigma_2}}S_{20}^*(-\omega)\sinh(\Gamma_0 z)\right] \times\exp(-\mathrm{i}D(\omega)z), \tag{33}$$

$$S_2^*(-\omega,z) = \left[S_{20}^*(-\omega)\cosh(\Gamma_0 z) + \mathrm{i}\sqrt{\frac{\sigma_2}{\sigma_1}}S_{10}(\omega)\sinh(\Gamma_0 z)\right] \times\exp(-\mathrm{i}D(\omega)z),$$

where $\Gamma(\omega) = \sqrt{\sigma_1\sigma_2}\,a_3^2 = \Gamma_0$ is the increment of the so-called stationary amplification (constant for all frequency components).

It thus becomes apparent that the OPA gain bandwidth becomes unlimited if the CXP has a particular angular dispersion described by Eqn (31), and, hence, the broadband chirped pulse experiences stationary amplification. The amplified signal and idler pulses [see Eqn (32)] travel locked together with the same group velocity and experience the opposite GVD. At the degeneracy, the GVD term vanishes.

As an example, consider type-I degenerate parametric amplification ($\omega_1 = \omega_2$, $k_{10} = k_{20}$, $v_{13} = v_{23}$, $g_{10} = g_{20}$) in a nonlinear crystal of length $z = L$ of the signal pulse, described by Eqn (24), with the angular dispersion $\delta^2(\omega)$ matching the condition of the infinite OPA gain bandwidth. The amplified pulse attains its shortest duration after propagating in the free space the distance z_c and its complex amplitude has the form

$$A_1(r,\eta,z_c) = \frac{B_0\cosh(\Gamma_0 L)}{2\pi}\int_{-\infty}^{\infty}\exp\left[-\left(\frac{\omega}{\Delta\omega}\right)^2\right] \times J_0(\delta_1(\omega)r)\exp(-\mathrm{i}\alpha\omega)\exp(\mathrm{i}\omega\eta)\mathrm{d}\omega, \tag{34}$$

where

$$\delta_1^2(\omega) = k_{10}g_{10}\omega^2;\quad z_c = \frac{2\beta}{n_1 g_{10}\Delta\omega^2};\quad \alpha = v_{13}L. \tag{35}$$

Here, α describes only the temporal shift of the compressed signal pulse occurring due to the group velocity mismatch and has no impact on the compression result.

Figure 8 illustrates the results of the numerical simulation of CXP amplification in non-critically type-I phase-matched LBO crystal at the degeneracy, with account for the third-order dispersion [22]. The input signal CXP with the central wavelength 1055 nm has a duration of 1 ps and a chirp parameter $\beta = 100$. These parameters correspond to a bandwidth-limited X-pulse of duration 10 fs. Figure 8a shows the amplified CXP, whose temporal on-axis profile remains Gaussian with a somewhat reduced temporal width (0.8 ps) due to gain narrowing caused by the finite (5 ps) pump pulse duration. The amplified CXP experiences self-compression during its propagation in the free space (or vacuum). The best compression occurs at $z = 125$ mm, yielding a highly localised X-shaped profile as plotted in Fig. 8b with the axial FWHM pulse duration of 26 fs. The compression dynamics versus the free-space propagation distance z is shown in Fig. 8c. Note that imperfect compression in terms of the pulse duration is due to uncompensated third-order dispersion imposed by the pulse propagation within the nonlinear crystal.

5. Conclusions

In this paper, we have shown that parametric amplification of the localised waves in the field of the intense pump with a quite different localisation level (X-pulse, pulsed Bessel beam or focused Gaussian beam) is generally possible due to simultaneous achievement of angular and spectral phase-matching requirements. We have demonstrated that the phase-locking of the temporal spectrum components comprising the X-pulse is readily achievable in the OPA in the case of the properly chosen pump geometry (e.g., Bessel or tightly focused Gaussian pump beam). As a result, a quasi-monochromatic pulsed Bessel beam is converted into a localised (e.g. non-diffracting and non-dispersing) X-pulse with a shorter pulse duration and a smaller beam waist. This happens due to azimuthal and radial correlations that arise in a quantum noise under parametric gain in the strong optical field of the Bessel beam central peak, while the phase-locking of the spatial components (transverse localisation) is resulted by non-collinear phase-matching in the nonlinear crystal. More generally, we note that the appearance of conical emission in the nonlinear optical processes can be considered as a signature of the formation of localised X-shaped wave packets.

As for possible future applications of the X-pulses in the field of high-intensity optics, the use of chirped X-pulses is of particular interest and promise an innovative approach in forthcoming applications. By means of a numerical experiment, we have demonstrated that the X-pulse with the properly chosen spatial and temporal chirp could be efficiently amplified in an OPA without phase distortions and could be self-compressed during propagation in the free space. This marks a new approach to the optical parametric chirped pulse amplification, OPCPA technique, suggesting a relevant simplification, because it does not require complex optical arrangement of the pulse compressor.

The main advantage of the optical parametric amplifiers in the domain of localised-wave optics is their potential capability of amplification and generation of the X-pulses in broad spectral range spanning from the ultraviolet up to the far infrared. Moreover, the carrier frequency and the angular dispersion of the X-pulse depends on the pump wavelength, the orientation of a nonlinear crystal and the phase-matching geometry. All these parameters might be continuously tunable, opening a possibility of involvement of OPAs in amplification and/or formation of localised X-

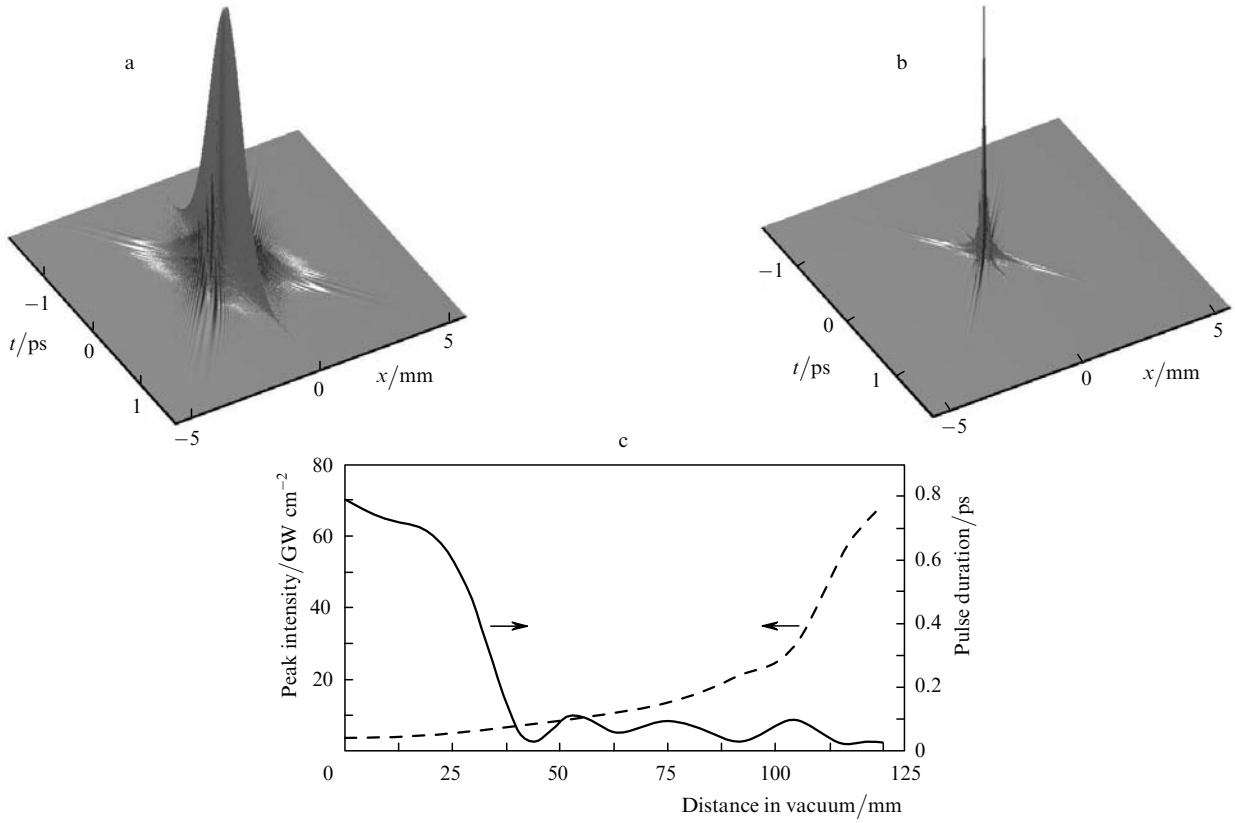

Figure 8. Spatiotemporal intensity distribution of (a) the amplified CXP pulse at the output of the nonlinear crystal, (b) after propagating the distance z_c in the free space; (c) dynamics of the axial FWHM duration (solid curve) and peak intensity of the amplified CXP propagating in a vacuum. Reprinted with permission from Ref. [22].

shaped wave packets with desirable spatial, temporal and propagation properties. It is worth noting that the unique properties of the OPA to sustain both very broad temporal and angular spectra envisage amplification of the polychromatic images of arbitrary three-dimensional structure [59] including different families of non-diffracting and non-dispersing envelope waves.

Acknowledgements. We consider it a privilege to have been invited to write the paper to this special issue devoted to the 80th birthday of Prof. S.A. Akhmanov. One of the coauthors of the present paper (A.P.) knew S.A. Akhmanov in person, being very close to him as his Ph.D. student in late 1960s and taking part in launching the first optical parametric amplifiers and oscillators. It was a real fortune to work in the laboratory under supervision of one of the pioneers of nonlinear optics and very generous person at the same time. The ideas shared out by Prof. S.A. Akhmanov still remain a driving force for scientific quests after his untimely death in 1991.

The authors wish to thank Dr. R. Butkus and Dr. S. Orlov (Vilnius University) in providing the part of experiments and computer simulations, respectively. Their coauthorship in quite a number of our common papers on the X-pulse OPAs is highly appreciated.

We also gratefully acknowledge the support from national and European projects at the Laser Research Center of Vilnius University: project FORTAS (No. B-29/2008) and Grant No. T-07-217 from the Lithuanian State Science and Studies Foundation, Project 'LASERLAB-Europe', Grant No. RII3-CT-2003-506350 under the European Commission (EC) 6th Frame-work Programme, and Projects 'LASERLAB-Europe Cont.', Grant No. 212025 and 'Extreme Light Infrastructure (ELI) Preparatory Phase', Grant No. 212105, both under EC 7th Framework Programme.

References

1. Akhmanov S.A., Khokhlov R.V. *Zh. Eksp. Teor. Fiz.*, **43**, 351 (1962) [*Sov. Phys. JETP*, **16**, 252 (1963)].
2. Kroll N.M. *Phys. Rev.*, **127**, 1207 (1962).
3. Kingston R. *Proc. IRE*, **50**, 472 (1962).
4. Akhmanov S.A., Kovrigin A.I., Piskarskas A.S., Fadeev V.V., Khokhlov R.V. *Pis'ma Zh. Eksp. Teor. Fiz.*, **2**, 300 (1965) [*JETP Lett.*, **2**, 191 (1965)].
5. Wang C., Racette G. *Appl. Phys. Lett.*, **6**, 169 (1965).
6. Giordmaine J.A., Miller R.C. *Phys. Rev. Lett.*, **14**, 973 (1965).
7. Akhmanov S.A., Kovrigin A.I., Kolosov V.A., Piskarskas A.S. *Pis'ma Zh. Eksp. Teor. Fiz.*, **3**, 372 (1966) [*JETP Lett.*, **3**, 241 (1966)].
8. Akmanov A.G., Akhmanov S.A., Khokhlov R.V., Kovrigin A.I., Piskarskas A.S., Sukhorukov A.P. *IEEE J. Quantum Electron.*, **QE-4**, 828 (1968).
9. Danielius R., Piskarskas A., Stabinis A., Banfi G.P., Di Trapani P., Righini R. *J. Opt. Soc. Am. B*, **10**, 2222 (1993).
10. Cerullo G., De Silvestri S. *Rev. Sci. Instr.*, **74**, 1 (2003).
11. Campillo A.J., Hyer R.C., Shapiro S.L. *Opt. Lett.*, **4**, 357 (1979).
12. Birmontas A., Piskarskas A., Stabinis A. *Kvantovaya Elektron.*, **10**, 1881 (1983) [*Sov. J. Quantum Electron.*, **13**, 1243 (1983)].
13. Gale G.M., Cavallari M., Hache F. *IEEE J. Sel. Top. Quantum Electron.*, **4**, 224 (1998).
14. Dubietis A., Jonusauskas G., Piskarskas A. *Opt. Commun.*, **88**, 437 (1992).

15. Ross I.N., Matousek P., Towrie M., Langley A.J., Collier J.L. *Opt. Commun.*, **144**, 125 (1997).
16. Wilhelm T., Piel J., Riedle E. *Opt. Lett.*, **22**, 1494 (1997).
17. Dubietis A., Butkus R., Piskarskas A. *IEEE J. Sel. Top. Quantum Electron.*, **12**, 163 (2006).
18. Lozhkarev V.V., Freidman G.I., Ginzburg V.N., Katin E.V., Khazanov E.A., Kirsanov A.V., Luchinin G.A., Mal'shakov A.N., Martyanov M.A., Palashov O.V., Potemkin A.K., Sergeev A.M., Shaykin A.A., Yakovlev I.V. *Laser Phys. Lett.*, **4**, 421 (2007).
19. Butkus R., Orlov S., Piskarskas A., Smilgevicius V., Stabinis A. *Opt. Commun.*, **244**, 411 (2005).
20. Orlov S., Piskarskas A., Stabinis A. *Opt. Lett.*, **27**, 2103 (2002).
21. Lagrange S., Jauslin H.R., Picozzi A. *Europhys. Lett.*, **79**, 64001 (2007).
22. Valiulis G., Dubietis A., Piskarskas A. *Phys. Rev. A*, **77**, 043824 (2008).
23. Hernandez-Figueroa H.E., Zamboni-Rached M., Recami E. (Eds) *Localized Waves* (Hoboken, NJ: John Wiley and Sons, 2007).
24. Durnin J., Miceli J.J., Eberly J.H. *Phys. Rev. Lett.*, **58**, 1499 (1987).
25. Saari P., Reivelt K. *Phys. Rev. Lett.*, **79**, 4137 (1997).
26. Conti C., Trillo S., Di Trapani P., Valiulis G., Piskarskas A., Jedrkiewicz O., Trull J. *Phys. Rev. Lett.*, **90**, 170406 (2003).
27. Porras M.A. *Opt. Lett.*, **26**, 1364 (2001).
28. Zamboni-Rached M., Shaaravi A.M., Recami E. *J. Opt. Soc. Am. A*, **21**, 1564 (2004).
29. Zamboni-Rached M., Hernandez-Figueroa H.E., Recami E. *J. Opt. Soc. Am. A*, **21**, 2455 (2004).
30. Besieris I.M., Shaaravi A.M. *Phys. Rev. E*, **72**, 056612 (2005).
31. Zapata-Rodriguez C.J., Porras M.A. *Opt. Lett.*, **31**, 3532 (2006).
32. Saari P., Reivelt K., Valtna H. *Laser Phys.*, **17**, 297 (2007).
33. Sonajalg H., Ratsep M., Saari P. *Opt. Lett.*, **22**, 310 (1997).
34. Grunwald R., Kebbel V., Neuman U., Rini M., Nibbering E.T.J., Piche M., Rousseau G., Fortin M. *Phys. Rev. A*, **67**, 063820 (2003).
35. Grunwald R., Griebner U., Tschirschwitz F., Nibbering E.T.J., Elsaesser T., Kebbel V., Hartmann H.-J., Jüptner W. *Opt. Lett.*, **25**, 981 (2000).
36. Shaarawi A.M., Besieris I.M., Said T.M. *J. Opt. Soc. Am. A*, **20**, 1658 (2003).
37. Valtna H., Reivelt K., Saari P. *Opt. Commun.*, **278**, 1 (2007).
38. Khilo A.N., Katranji E.G., Ryzhevich A.A. *J. Opt. Soc. Am. A*, **18**, 1986 (2001).
39. Kutz J.N., Conti C., Trillo S. *Opt. Express*, **15**, 16022 (2007).
40. Conti C., Trillo S. *Opt. Lett.*, **28**, 1251 (2003).
41. Di Trapani P., Valiulis G., Piskarskas A., Jedrkiewicz O., Trull J., Conti C., Trillo S. *Phys. Rev. Lett.*, **91**, 093904 (2003).
42. Jedrkiewicz O., Trull J., Valiulis G., Piskarskas A., Conti C., Trillo S., Di Trapani P. *Phys. Rev. E*, **68**, 026610 (2003).
43. Longhi S. *Phys. Rev. E*, **69**, 016606 (2004).
44. Orlov S., Stabinis A., Smilgevicius V., Valiulis G., Piskarskas A. *Opt. Lett.*, **32**, 68 (2007).
45. Kolesik M., Wright E.M., Moloney J.V. *Phys. Rev. Lett.*, **92**, 253901 (2004).
46. Couairon A., Gaizauskas E., Faccio D., Dubietis A., Di Trapani P. *Phys. Rev. E*, **73**, 016608 (2006).
47. Faccio D., Averchi A., Couairon A., Kolesik M., Moloney J.V., Dubietis A., Tamosauskas G., Polesana P., Piskarskas A., Di Trapani P. *Opt. Express*, **15**, 13077 (2007).
48. Faccio D., Di Trapani P. *Laser Phys.*, **18**, 253 (2008).
49. Longhi S., Janner D. *Phys. Rev. B*, **70**, 235123 (2004).
50. Lahini Y., Frumker E., Silberberg Y., Droulias S., Hizanidis K., Morandotti R., Christodoulides D.N. *Phys. Rev. Lett.*, **98**, 023901 (2007).
51. Kevrekidis P.G., Gagnon J., Frantzeskakis D.J., Malomed B.A. *Phys. Rev. E*, **75**, 016607 (2007).
52. Clerici M., Jedrkiewicz O., Rubino E., Faccio D., Tartara L., Degiorgio V., Di Trapani P. *Opt. Lett.*, **33**, 2296 (2008).
53. Di Trapani P., Berzanskis A., Minardi S., Sapone S., Chinaglia W. *Phys. Rev. Lett.*, **81**, 5133 (1998).
54. Di Trapani P., Valiulis G., Chinaglia W., Andreoni A. *Phys. Rev. Lett.*, **80**, 265 (1998).
55. Marcinkevicius A., Piskarskas A., Smilgevicius V., Stabinis A. *Opt. Commun.*, **158**, 101 (1998).
56. Piskarskas A., Smilgevicius V., Stabinis A., Vaicaitis V.J. *Opt. Soc. Am. B*, **16**, 1566 (1999).
57. Valiulis G., Dubietis A., Danielius R., Caironi D., Visconti A., Di Trapani P. *J. Opt. Soc. Am. B*, **16**, 722 (1999).
58. Porras M. A., Valiulis G., Di Trapani P. *Phys. Rev. E*, **68**, 016613 (2003).
59. Lantz E., Devaux F. *IEEE J. Sel. Top. Quantum Electron.*, **14**, 635 (2008).